Journal of Materials Chemistry A

ROYAL SOCIETY OF CHEMISTRY

PERSPECTIVE

View Article Online
View Journal | View Issue

Cite this: J. Mater. Chem. A, 2020, 8, 22557

Towards accelerated durability testing protocols for CO_2 electrolysis†

U. O. Nwabara, [a] M. P. de Heer,[b] E. R. Cofell,[ac] S. Verma,[d] E. Negro[b] and Paul J. A. Kenis *[a]

Received 3rd September 2020
Accepted 19th October 2020

DOI: 10.1039/d0ta08695a

rsc.li/materials-a

In recent years, the electrochemical reduction of CO_2 (ECO_2RR) to value-added chemicals, fuels, and intermediates has been proposed as a promising option for utilizing excess CO_2 emissions. ECO_2RR could be integrated into existing CO_2-emitting industrial processes to mitigate emissions. To get to that stage, however, ECO_2RR cells and systems need to exhibit lifetimes of thousands of hours, similar to other commercially viable electrochemical systems. Accelerated durability testing (ADT) has been employed to rapidly screen the stability of these other electrochemical systems. Currently, most ECO_2RR studies only report durability for tens of hours. Yet, once the ECO_2RR field reaches longer system lifetimes as a whole, ADT studies will become necessary. In this perspective, we evaluate accelerated durability studies employed for fuel cells, water electrolyzers, and chlor alkali systems and apply the knowledge to suggest an appropriate ECO_2RR ADT protocol, which is currently lacking.

1. Introduction

Each year, the world releases an extra 14.7 Gt of CO_2, meaning natural processes and phenomena (photosynthesis, oceans, *etc.*) have surpassed their CO_2 uptake capacity.[1,2] Additionally, growing populations, especially in developing countries, will contribute to an increase in the demand of energy (electricity production), fuels (petroleum refining), materials (deforestation), amongst other resources, which collectively contribute to total CO_2 emissions.[3] Electricity generation and transportation alone make up 68% of all CO_2 emissions.[4] If left untreated, high atmospheric (and oceanic) CO_2 concentrations will continue to negatively impact the earth's temperatures and various ecosystems.[5]

Various solutions have been proposed to reduce CO_2 emissions such as carbon capture and sequestration, battery-electric vehicles, and higher efficiency coal-fired/natural gas power plants. Over the last 30+ years, researchers have investigated the electrochemical reduction of CO_2 (ECO_2RR) to value-added chemicals, fuels, and intermediates such as carbon monoxide (CO), ethanol, ethylene, formic acid, methane, and methanol.[6] Hori's work summarized which transition metal cathode catalysts show activity for ECO_2RR and the products they make.[7] For instance, Au and Ag produce CO at high faradaic efficiencies (FE) while Cu is the only metal that makes hydrocarbons and oxygenates. Although, more recent studies have investigated nontraditional, carbon-based catalysts for ECO_2RR.[8]

A variety of configurations such as three-electrode cells and flow electrolyzers have been used to study promising catalysts and operating conditions for ECO_2RR.[9–11] Regardless of the configuration chosen, the lab-scale device must perform well in all of the following metrics for the ECO_2RR technology to be considered for industrial-scale application. These metrics include high current density (activity), low overpotentials (high energy efficiency), high product faradaic efficiency (selectivity), and extensive durability/stability. Technoeconomic analyses have been carried out to define benchmarks for all of the above metrics.[12–14] When considering economic feasibility, high selectivities (>80%) become of high importance when needing to purify products downstream as separations become less expensive at higher concentrations. Moreover, high current densities ($\geq$300 mA cm^{-2}) when combined with high FE correspond to a larger amount of desired products being formed. Low overpotentials (at both the cathode and anode) translate to high energy efficiency and therefore low energy requirements for the entire reaction. As the energy input declines, so does the costs. Finally, an unstable, non-durable system requires frequent replacement of the catalysts and other materials, which increases cost.

The vast majority of the work to date in the ECO_2RR field has focused on developing selective and active catalysts for various products with notable success.[15–20] However, few publications

[a]Chemical and Biomolecular Engineering, University of Illinois at Urbana-Champaign, 600 S Mathews St, Urbana, IL 61801, USA. E-mail: kenis@illinois.edu

[b]Shell Global Solutions International B.V., Grasweg 31, 1031 HW Amsterdam, The Netherlands

[c]Material Science and Engineering, University of Illinois at Urbana-Champaign, 1304 W Green St, Urbana, IL 61801, USA

[d]Shell International Exploration and Production Inc., 3333 Highway 6, South Houston, TX-77082, USA

† Electronic supplementary information (ESI) available. See DOI: 10.1039/d0ta08695a

have sustained these necessary selectivities and activities for suitable lifetimes. Technoeconomic analyses on ECO_2RR concluded that a feasible electrolyzer should exhibit stable performance for at least 3,000 h with some stating a need for at least 20,000 h.[12–14] Although these studies do not define a specific performance target when outlining these benchmarks, staying within 25% of initial performance (*i.e.*, energy and faradaic efficiency) would be paramount for economic viability and agrees with targets set for proton exchange membrane (PEM) water-splitting electrolyzers and other commercial electrochemical systems. Actually, end-of-life in a fuel cell has been defined as performance dropping by more than 10%.[21] Yet, the definition for end-of-life is open to interpretation. For ECO_2RR, achieving higher durability can be difficult due to an assortment of degradation mechanisms at play that lead to a drop in performance. The majority of published durability studies report lifetimes of less than 100 h.[22–25] To date, only few studies have reported a system durability (when considering a drop in performance of up to 10%) greater than 1000 h, producing CO (or syngas) as the main product.[10,20]

Developing a durable, stable ECO_2RR system requires monitoring the reaction for countless hours; for example, 1000 h is equal to 1.5 months of testing. Testing a system for this duration to determine its durability is impractical. To characterize the durability of any electrochemical system in a timelier manner, researchers have turned to accelerated durability and stress tests (ADT and AST, respectively). In an accelerated study, a certain aspect of the system (catalyst, membrane, electrode, *etc.*) or the entire system is subjected to conditions that expedite degradation and therefore shorten the durability study. The system's lifetime can then be inferred upon completing an ADT or AST. At times, ADT and AST are used interchangeably. ADT specifically assesses system durability at an accelerated rate while AST stresses systems by subjecting them to extreme conditions to study robustness. ASTs are commonly utilized to mimic variable load cycling systems as fuel cell research when considering variable loads. Moreover, ADTs are more relevant for technologies that operate at the same rate over long periods of time like ECO_2RR. A comparison between ADTs and ASTs is given in Table S1.†

Several recent ECO_2RR research efforts have focused on identifying degradation mechanisms that hinder durability in real time over a timescale of one to tens of hours.[15,26,27] These mechanisms hamper ECO_2RR and eventually cause system failure, as we discussed recently in a review.[28] Upon recognizing and understanding these failure mechanisms, better materials can be selected and better electrodes or overall systems can be designed to improve lifetimes. Once stability over tens of hours is achieved across the ECO_2RR field, for instance retention of 90% of performance after 48 hours, ADTs and standardized ADT protocols are required.

The goal of this perspective is to arrive at an ADT protocol to characterize the durability of catalysts and cathodes for ECO_2RR. First, we briefly summarize catalyst- and electrode-related causes for loss in performance. Then, we examine ADTs and ASTs developed for other electrochemical systems, such as fuel cells, chlor alkali electrolysis, and water electrolysis. Based on this prior work and the specific characteristics and demands of ECO_2RR, we propose an ADT protocol for CO_2 electrolysis.

2. Causes of ECO_2RR performance loss

A variety of issues can diminish the performance of an ECO_2RR system and subsequently can cause instantaneous or gradual failure. Fig. 1 summarizes key issues that researchers have come across whilst carrying out durability studies. These listed mechanisms consider the use of a gas diffusion electrode (GDE, *i.e.*, a catalyst layer deposited on carbon paper or a gas diffusion layer) since most ECO_2RR studies that reach high current densities use a GDE-based configuration.[28] Several of these mechanisms occur in other types of electrode substrates such as glassy carbon, meshes, and carbon cloths, *etc*. In addition, other components of a system, such as membranes, can experience degradation.

Leaching, poisoning, and aggregation are processes that are specific to the catalyst layer and prompt a decline in electrolysis performance *via* one or more of the four metrics mentioned above. First, catalyst particles can detach from the layer and leach into the electrolyte solution, thus losing their ability participate in ECO_2RR. Second, adsorbates (*e.g.* reaction intermediates and impurities from the electrolyte) that bind strongly to the active sites can poison the catalyst, in effect blocking the active sites from ECO_2RR. Third, upon electrolysis the particles in the catalyst layer can begin to aggregate, decreasing the amount of accessible active sites.

Beyond just the catalyst layer, binder dissolution can affect the entire electrode. The binder holds the contents of each of the layers in the GDE together and provides the hydrophobicity/hydrophilicity needed to maintain ideal gas/liquid phase separation. Typical binders include fluorinated polymers that with proper water management properties, such as Nafion and PTFE. However, when exposed to ECO_2RR electrolytes, especially alkaline electrolytes employed to improve reaction kinetics, these binders can break down, leading to their dissolution.[29,30] Flooding of the electrode often stems from binder dissolution (or binder degradation leading to dissolution) and loss of hydrophobicity in the GDE. The aqueous electrolyte can then seep into the gas diffusion layer and ultimately impedes CO_2

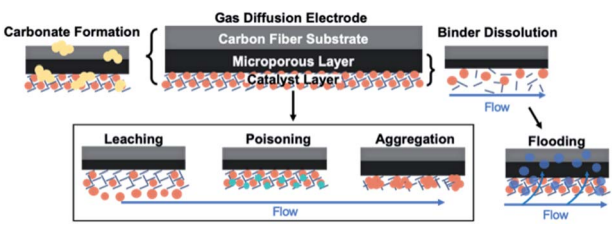

Fig. 1 Common electrode failure mechanisms observed by researchers studying ECO_2RR including carbonate formation, binder dissolution, catalyst leaching, catalyst poisoning, and catalyst aggregation. Binder dissolution can cause flooding in the entire electrode.

from reaching the catalyst, therefore hampering ECO_2RR. At that time, unwanted carbonate formation and the hydrogen evolution reaction (HER) can start to occur (discussed below).

Carbonate formation, which intensifies when the electrode has flooded, can affect all layers of the GDE. In aqueous solutions, especially alkaline, CO_2 will react with water or hydroxide ions in an equilibrium reaction (eqn (1)–(3)) to form carbonate (and bicarbonate), which can precipitate on the electrode surface and in the pores; this can lead to blockages in the pores and impede CO_2 from reaching the catalyst layer.[31]

$$CO_2\ (aq) + H_2O\ (l) \rightleftharpoons H_2CO_3\ (aq) \quad K = 10^{-6} \tag{1}$$

$$CO_2\ (aq) + OH^- \rightleftharpoons HCO_3^-\ (aq) \quad K = 4 \times 10^7 \tag{2}$$

$$HCO_3^-\ (aq) + OH^- \rightleftharpoons CO_3^{2-}\ (aq) + H_2O\ (l) \quad K = 10^3 \tag{3}$$

Once initiated, all of the mechanisms depicted in Fig. 1 can enhance HER. Hydrogen evolution decreases FE for desired products by taking current meant for ECO_2RR and producing H_2. For example, leaching, binder dissolution, and aggregation expose the carbon of the GDE substrate to the aqueous electrolyte, and thus can catalyze HER. Moreover, certain adsorbates on the catalyst surface may catalyze HER, *e.g.*, trace metals from the electrolyte solution. Either way, current devoted to ECO_2RR is lost to an unwanted side product. HER requires less energy (lower equilibrium potential) than ECO_2RR, and therefore is accompanied by an increase in cell potential (less negative).

Researchers utilize a wide range of characterization methods to assess the behavior of catalysts and electrodes over time, identifying which failure mechanisms occur during extended operation.[28] Similar characterization methods will need to be employed in ADTs and ASTs.

3. Accelerated stress and durability testing methods and protocols developed for other major electrochemical processes

The United States Department of Energy (DOE) has developed and periodically updates ADT/AST protocols for testing the various aspects of proton exchange membrane fuel cells (PEMFC).[32] In a similar vein, AST and ADT methods have been developed for other electrochemical applications, including water electrolysis and chlor-alkali electrolysis.[33–40] ASTs and ADTs help to determine the degradation mechanisms of different parts of an electrochemical system, especially the electrocatalysts, catalyst ionomer/binder, and ion exchange membrane. Knowledge gained from such studies has improved the performance in terms of durability, and therefore the techno-economic feasibility, of several of the aforementioned applications and has led to significant strides towards achieving their respective durability targets.

At present, the ECO_2RR field lacks common protocols for ADT. As discussed above, ECO_2RR systems have not met durability targets needed for their application at scale. In this

Table 1 Summary of accelerated durability tests performed for electrochemical process than ECO_2RR. The table details the exact degradation mechanism and the type(s) of tests and characterization methods used to identify them

		Characterization method					
Degradation mechanism	Result of degradation	Technique	*In situ*	*Ex situ*	Type of accelerated durability	Shape of degradation curve	References
Physical							
Aggregation, agglomeration	Decrease in ECSA	SEM		✓	Potential or current cycling	Linear	36, 41 and 42
	Decrease in reaction rate/ activity	TEM		✓			
		CV	✓				
	Decrease in cell performance	Electroanalysis	✓				
		XRD		✓			
Delamination (MEA)	Increase in high frequency cell resistance	Milliohm meter	✓		Steady state current or potential	Step drop	35
Membrane breaking	Cell failure	NMR		✓	Humidity cycling	Step drop	43
		Fluoride emissions	✓				
		Tensile tests		✓			
Electrode wetting	Decrease in cell performance	Electron probe microanalysis		✓	Steady state current or potential	Linear	37
Chemical							
Binder degradation	Decrease in cell performance	XPS		✓	Potential or current cycling Steady state current or potential	Linear	42 and 44
Carbon corrosion/ oxidation	Decrease in cell performance	XPS		✓	Potential or current cycling Steady state current or potential	Linear	40 and 42

section, we review the protocols and AST & ADT methods for fuel cells, chlor-alkali electrolyzers, and water electrolyzers, applications that are (well) ahead of ECO_2RR in their development. Table 1 summarizes common failure mechanisms, types of testing, and the characterization techniques for these applications.

3.1 Fuel cells

3.1.1 State of the art durability testing protocols for PEMFCs. A major driver for fuel cell research and design was the genesis of space programs and exploration in the 1950s.[45] Today, PEMFCs are being designed for mobility and power applications. With the goal of implementing PEMFCs for such applications, labs under the U.S. Department of Energy (*i.e.,* National Renewable Energy Laboratory, NREL) have established durability targets (all >5000 h) for PEMFCs.[21] Each year, NREL releases progress reports compiling the relative published work to compare to these targets. A majority of the data from these reports was collected from accelerated testing studies. As a way to regulate these accelerated studies and simplify data compilation, DOE developed standard AST protocols to test different aspects of a PEMFC including the electrocatalyst, catalyst support, and membrane.[32]

The main components of the DOE protocols are the type & number of cycles, applied potential or current, operating conditions, and the fuels/reactants used. Table 2 summarizes the electrocatalyst testing protocol including the specific operating conditions and performance metrics and targets. The metric(s) that are measured during the durability tests depend on the cell feature being studied. The type of a test cycle employed for a PEMFC depends on whether the desire is to test the system in startup/shutdown mode (*i.e.*, car ignition), which corresponds to triangle or step cycles, or run mode (*i.e.*, driving), which corresponds to constant potential/current.[46] In a version of this AST/ADT protocol adapted for ECO_2RR, a constant potential/current (steady state) would be used for continuous production, while step/triangle cycles would mimic starting/stopping of CO_2 electrolyzers. Metrics would include faradic efficiency, energy efficiency, and activity.

The same DOE report published protocols listing the exact steps to run when determining cell or stack durability and polarization curves.[32] Such methods and protocols can be optimized for durability testing of other electrochemical systems. Indeed, the DOE has working groups and focus areas for these other electrochemical process (water electrolysis, CO_2 electrolysis, *etc.*) through its various offices, often with significant involvement of the National Labs.[47,48]

3.1.2 Accelerated studies for fuel cells. PEMFCs have a wide range of applications. Depending on the intended application, AST/ADT will be performed under steady state or cyclic conditions to determine relevant chemical and mechanical degradation mechanisms.

Selection of appropriate characterization techniques, whether *in situ* or *ex situ*, is also crucial for revealing what occurs during operation. For example, Vaarmets *et al.* adapted the DOE PEMFC protocol to run 30 000 cycles on Pt nanoparticle-activated carbide derived carbon using scanning electron microscopy (SEM), transmission electron microscopy (TEM), cyclic voltammetry (for electrochemical surface area), and X-ray diffraction (for crystallite growth) to determine the underlying reason for any change in performance.[41] Triangular cycles with a potential range from 0.6–1.0 V and a scan rate of 30 mV s^{-1} were used. The characterization techniques revealed an increase in average Pt particle diameter after the 30 000 cycles (Fig. 2), corresponding to a decrease in electrochemical surface area (ECSA): a decrease of 21% alone in the first 3000 cycles. The authors concluded that the main degradation mechanisms occur within the first 10 000 cycles, after which the ECSA of the catalyst and electrode surface stabilized.

In earlier work, some of us carried out a cyclic accelerated long-term stability study over 6000 cycles with a range of 0.535 to 1.035 V, but in an alkaline three-electrode fuel cell. Polarization curves showed first a rapid and then a gradual decrease in reaction rate as more cycles were completed, presumably indicating multiple degradation regimes over various time scales (further analysis needed to determine which ones).[49] Degradation regimes reveal the mechanisms occurring in any electrochemical system including ECO_2RR. Rather than using a potential range, Zhang *et al.* executed a 300 h ADT of a PEMFC

Table 2 Summary of DOE AST method for testing the stability of the electrocatalyst in a PEMFC. The top half details the operating conditions for the test while the bottom half lists the metrics, frequency of measurements, and desired performance targets. Adapted from ref. 32

Cycle	Triangle sweep cycle: 50 mV s^{-1} between 0.6 V and 1.0 V. Single cell 25–50 cm^{-2}
Number	30 000 cycles
Cycle time	16 seconds
Temperature	80 °C
Relative humidity	Anode/cathode humidity 100/100%
Fuel/oxidant	H_2/N_2 (H_2 at 200 sccm and N_2 at 75 sccm for 50 cm^2)
Pressure	Atmospheric pressure

Metric	Frequency of measurement	Performance target
Catalytic mass activity	At the beginning and end of test minimum	<40% loss of initial catalytic activity
Polarization curve from 0 to >1.5 A cm^{-2}	After 0, 1k, 5k, 10k, and 30k cycles	<30 mV loss at 0.8 A cm^{-2}
ECSA/cyclic voltammetry	After 10, 100, 1k, 3k, 10k, 20k, and 30k cycles	<40% loss of initial area

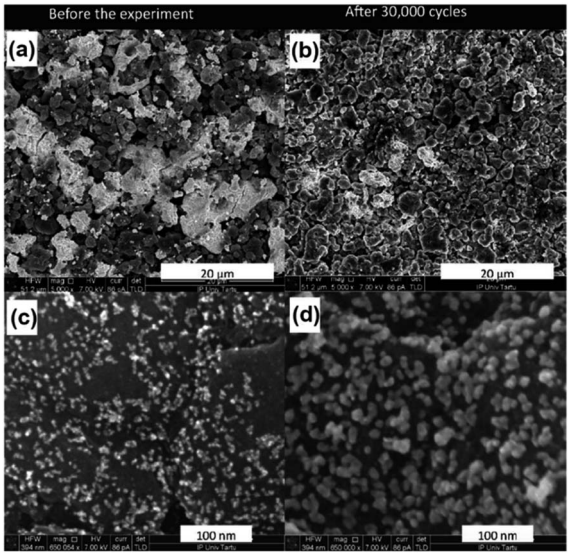

Fig. 2 High resolution SEM of Pt nanoparticles subjected to accelerated durability testing; (a) and (c) show particles before electroanalysis and (b) and (d) after 30 000 cycles in a PEMFC. The average Pt particle size increased after the completion of cycles. Reproduced with permission from ref. 41.

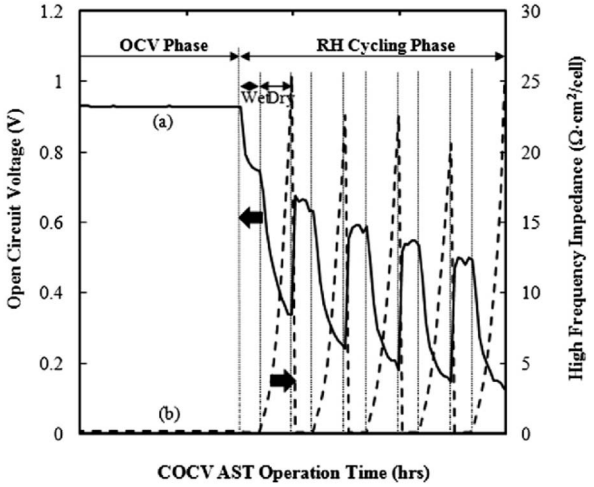

Fig. 3 AST of a PEMFC performed by cycling between wet and dry inlet gases with the corresponding open circuit voltage and high frequency impedance. Reproduced with permission from ref. 43.

using two current ranges.[42] A single cycle involved running at high current densities (0.6 to 1.0 A cm^{-2}) for 60 min and then lower current densities (0.2 to 0.5 A cm^{-2}) for 60 minutes separated by 10 minute holds at open circuit voltage (OCV). This study employed X-ray Photoelectron Spectroscopy (XPS) to distinguish an overall decrease in fluorine, especially in $CF_{x>1}$ groups, due to ionomer degradation. Notably, an increase in oxidized carbon species (C–O and C═O) was observed in XPS, interpreted as oxidation of the carbon support of the Pt catalysts. This oxidation can lead to separation of Pt from the support and agglomeration, both of which decrease cell performance. Unwanted hydrogen peroxide formation is another issue that can occur at the cathode.[50] Both carbon supports and fluorinated ionomers (binders) can be used to create electrodes for use in ECO_2RR, so such techniques can be implemented for ECO_2RR AST and ADT.

In a slightly different approach, Lim *et al.* performed a cyclic accelerated stress test for a polymer electrolyte/membrane electrode assembly fuel cell by cycling the water content of the membrane (saturated *vs.* dry) instead of the potential.[43] This experiment monitored changes in OCV over time while varying the humidity of the inlet gases to study the chemical and mechanical degradation of the membrane (Fig. 3). Nuclear Magnetic Resonance (NMR) spectroscopy and fluoride emission measurements helped to show side- and main-chain degradation of the membrane. In addition, tensile tests revealed that the membrane became stiffer and more brittle over time. Ultimately, the membrane failed after 160 hours of operation when a pinhole formed in the membrane caused by the repeated swelling and shrinking of the membrane during the wet and dry cycles, respectively. Membranes are utilized in MEA-based electrolyzers and sometimes flow electrolyzers for ECO_2RR. Moreover, the chemical makeup for such membranes is similar to the binders/ionomers utilized in electrodes for ECO_2RR. Therefore, Lim's results give insight to possible membrane and electrode degradation such as swelling and binder dissolution.

An ADT/AST can also be conducted under steady state (non-cyclic) conditions by holding the current or potential constant at extreme conditions such as high temperatures and/or pressures and doubled or even tripled current/potential. Again, steady state conditions are more suitable for industrial ECO_2RR systems as they would likely be implemented for continuous production. Wagner *et al.* performed a durability test in an alkaline fuel cell by applying a constant current density of 100 mA cm^{-2} for more than 2500 hours.[44] By taking OCV electrochemical impedance spectroscopy (EIS) measurements at specific experiment times, the authors were able to discern how the degradation mechanisms/regimes were changing over time, similar to the aforementioned work by Brushett *et al.*[49] This experiment also employed XPS to study the cathode and found that the fluorine concentration decreased during the experiment, which was attributed to the decomposition of the polytetrafluoroethylene (PTFE) binder. Brushett *et al.* also conducted a steady state ADT on an alkaline fuel cell by keeping a constant cathode potential of 0.535 V *vs.* RHE for 24 hours.[49] They concluded that the most significant loss of activity occurred within the first 14 hours, viewing a similar electrode stabilization as Vaarmets *et al.* over a longer time.[41]

3.2 Accelerated studies for water electrolyzers

Water electrolysis involves the splitting of H_2O to obtain H_2. The ASTs and ADTs created for water electrolyzers are similar to those for fuel cells. For example, Siracusano *et al.* ran a 1000 h steady state durability test to determine the effect of two different variables, catalyst loading and applied current density, on the rate of catalyst degradation.[34] Ir + Ru electrodes of different loadings (0.34 and 1.27 mg cm^{-2}) were submitted to 1000 h of operation at two different current densities (1 and 3 A

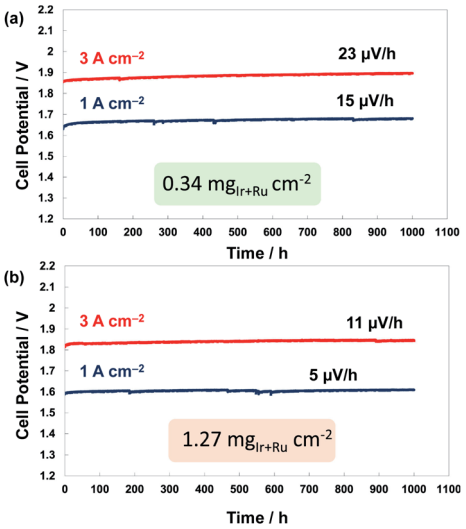

Fig. 4 Steady state durability tests of a water electrolyzer at a catalyst loading of (a) 0.34 mg cm^{-2} and (b) 1.27 mg cm^{-2} at different applied current densities. The slope from a linear fit of the curves can be interpreted as a catalyst degradation rate. Adapted with permission from ref. 34.

cm^{-2}). Catalyst loading also plays a large role in ECO_2RR in determining whether a system is in a kinetically or mass transport limited regime. As shown in Fig. 4, linear fits of the resulting curves provided degradation rates, revealing that degradation was faster at lower loadings and higher current densities. Combining this experiment with subjecting the electrodes to a corrosive electrolyte, Siracusano suggested three main variables that drive electrode corrosion: operating pH, operating temperature, and applied potential/current, all of which are important to ECO_2RR as well.

Leng *et al.* showed that the catalyst layer ionomer and the water feed configuration play a significant role in the durability of a solid-state water electrolyzer.[35] A constant 200 mA cm^{-2} (at 50 °C) was applied for more than 535 h while using a robust poly(sulfone) backbone-based ionomer in the catalyst layer and a water-fed (humid) anode. Measuring the high frequency cell resistance detected delamination of the catalyst layer from the membrane. A similar ADT can be applied to ECO_2RR experiments conducted with solid oxide electrolysis cells (SOECs) or membrane electrode assembly-(MEA) based cells.[10,19,51,52]

As mentioned previously, accelerated stress testing involves subjecting a cell component to extreme conditions, and such testing can be done outside of normal electrochemical cell configurations. For example, Paciok *et al.* employed an alternative setup to study electrode degradation.[36] In their AST experiments, a Pt-coated TEM grid was submerged in an acidic electrolyte for either 24 or 168 hours while 0.0, −0.1, or −0.2 V *vs.* RHE was applied. TEM measurements helped the authors observe cathode degradation *via* the mobility of carbon-supported Pt. Post-experiment TEM images revealed that when potentials were applied, the Pt particles migrated from their carbon supports and agglomerated, therefore lowering the ECSA and catalyst activity. They concluded that hydrogen absorbs on Pt and forms a monolayer, which encourages release of Pt particles from their carbon supports. Utilizing an AST based on this study for ECO_2RR can allow one to observe the robustness and degradation modes of a catalyst or electrode outside of a traditional ECO_2RR electrolyzer.

In summary, several ADTs and ASTs developed for water electrolysis, regardless of the configuration and operating conditions, offer potential techniques for ECO_2RR application.

3.3 Accelerated studies for chlor-alkali electrolysis

Chlorine has been produced for use in the textile and paper industries *via* the electrolysis of an aqueous chlorinated salt (*i.e.*, NaCl) since the mid-19th century.[53] Therefore, the durability and degradation of chlor-alkali processes has been studied extensively. Sugiyama *et al.* conducted experiments to study the degradation of GDEs in a chlor-alkali flow electrolyzer.[37] The electrode consisted of a Ag/carbon catalyst layer, a carbon gas supply layer, and a Ag mesh current distributing layer. The first experiment was a normal long-term durability test at constant current (300 mA cm^{-2}) that monitored the cell overpotential (η) over 1200 days (3 years). Using electron probe microanalysis to identify Na^+ ions in the electrode, the authors found that the observed rise in η was related to the wetting depth of the electrode by the electrolyte. Next, the authors pursued two approaches to accelerate the standard long-term case. In one accelerated case running for 62 days, the temperature, current density (600 mA cm^{-2}), and catholyte concentration were increased, while in the other accelerated case running for 32 days, the O_2 concentration of the cathode gas feed was lowered. O_2 depolarized cathodes reduce energy consumption for chlor alkali electrolysis compared to H_2 evolving cathodes.[38] In both accelerated cases, η increased over time, but by different amounts. Wetting depth was the source of degradation for both cases. In addition, higher potentials favored H_2O_2 formation, which can oxidize (degrade) the carbon materials in the gas supply layer. Three correlations were created using the results from all of these experiments: $\Delta\eta$ *vs.*

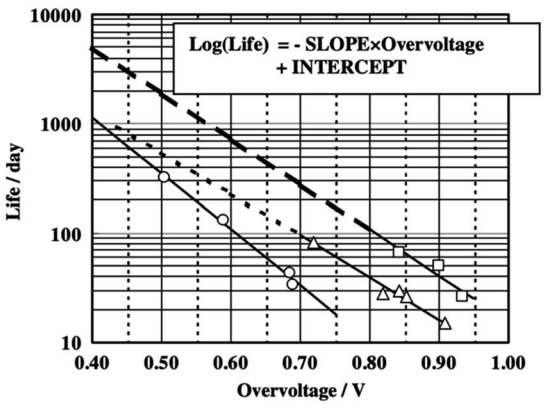

Fig. 5 Linear correlations derived from both long-term and accelerated durability data of various Ag electrodes for chlor-alkali electrolysis to estimate the life of certain electrode configurations. Reproduced with permission from ref. 37.

wetting depth (linear), η *vs.* O_2 concertation (logarithmic), and finally, estimated lifetime *vs.* initial η (linear, Fig. 5). This last correlation allowed the electrode lifetime (time for $\Delta\eta$ to reach 0.75 V) for the latter accelerated case to be estimated as 630 days (1.7 years).

Progressive electrolyte wetting can also be an issue for ECO_2RR flow electrolyzers, as it is the first step towards cell flooding, leading to similar failure modes as observed by Sugiyama *et al.* in chlor-alkali electrolysis. Moreover, correlations that relate degradation rate *vs.* an electrode property (like wetting depth for chlor-alkali) and electrode lifetime *vs.* degradation rate would be desired results of accelerated durability studies for ECO_2RR.

The durability of various chlor-alkali electrolyzers was discussed in a review by Moussallem *et al.*[38] One major takeaway was the exceptional stability observed for Ag-based electrodes when directly compared to standard Pt-based electrodes, which was reiterated in many of the included studies. For example, in one of the studies mentioned, Ag electrodes proved to be more stable, lasting over three times longer than Pt (>1000 days *vs.* 350 days).[39] Another study concluded that Ag outperforms Pt because Pt also catalyzes the oxidation of the carbon substrate, leading to a loss in contact between Pt and C.[40] Catalyst choice is imperative for all electrochemical processes including ECO_2RR, and studying catalyst stability aids in refining catalyst and support design to improve overall performance.

In an swashbuckling accelerated aging test, Sudoh *et al.* first ran polarization-curves and AC impedance measurements with the working electrode (1 hour) and then proceeded to boil it in 30 wt% NaOH (2 h); these steps were repeated for up to 22 h.[46] Over the 22 h testing period, both the charge transfer resistance (related to catalyst consumption) and double-layer capacitance (related to wettability) increased. From this experiment, the authors were able further understand the stabilities of their catalyst's active sites and their electrode's hydrophobicity. Here again we see an example of an AST performed outside of a typical cell configuration that supplied key information regarding catalyst and/or electrode stability.

In summary, these various AST and ADT efforts for chlor-alkali electrolysis provided highly useful insights and ideas towards developing proper acceleration techniques and data analysis approaches for ECO_2RR.

4. Accelerated durability testing protocol for ECO_2RR

Examining the accelerated studies for fuel cells, water electrolyzers, and chlor-alkali electrolyzers exposed a broad range of methods, techniques, and experiments that can be applied for the accelerated testing of ECO_2RR electrolyzers. Both ECO_2RR and the other electrochemical processes examined in Section 3, however, have been studied in a variety of different cell configurations. Thus, tests for one configuration may not apply or will not be comparable to others. As a result, having a single ECO_2RR accelerated testing protocol applicable to any system becomes paramount. In addition, being able to accurately compare results of both standard and accelerated ECO_2RR durability tests across various research groups would further help drive the field to standardized assessment of different options, enabling commercialization. In this section, we first present a durability operating procedure for benchmarking a system prior to running ADTs studies along with performance goals for standard durability (Table 3, Table S2†). Taking into account both the knowledge gained from AST/ADT for other electrochemical technologies (Section 3) and our understanding of ECO_2RR systems, we then propose an accelerated durability testing protocol for ECO_2RR (Table 4), heavily inspired by the DOE fuel cell protocol. The subsequent sections will outline the options for acceleration in addition to ways of characterizing the various failure mechanisms during and after testing.

4.1 Benchmark standard durability test for setup validation

As stated in the introduction, the ECO_2RR field must reach longer durability lifetimes as a whole before ADTs/ASTs are commonly integrated into regular lab-scale setups. Such lifetimes should also be exhibited under industrially relevant current densities ($\geq$200 mA cm^{-2}) and ideally using scalable ECO_2RR cell configurations (flow cell, MEA). Basically, an ECO_2RR configuration should try and meet a preestablished durability performance benchmark before beginning to undergo routine ADT testing. With this, comparing ECO_2RR performance across various labs becomes easier and more impactful. Like the standard durability protocol described in our literature review,[28] here we lay out a standard operating procedure for benchmarking one's ECO_2RR system to ensure it is suitable for accelerated studies.

Table 3 specifies materials, operating conditions, and steps to follow before, during, and after durability testing. A flow chart of these steps is provided in Fig. S1.† The table is divided by characterization, conditioning, and durability testing. Prior to running the durability test, the electrode and electrolyte should be characterized to obtain information on morphology and composition as a reference for post-testing characterization. The electrode and membrane have to be conditioned prior to the test as well. The membrane needs to be soaked in a hydroxide-based electrolyte to exchange any pre-doped anions with OH^-, which is generated during ECO_2RR and shuttled to the anode. *In situ* or *ex situ* conditioning of the cathode rids the catalyst surface of any pre-formed oxides that may sully results. The durability test involves holding the assembled cell at a constant current (or potential) while continuously monitoring performance. Once the durability test has concluded, the initial characterization techniques should be repeated in addition to data analysis to measure CO_2 conversion and crossover, if applicable.

When benchmarking a system for accelerated studies, we propose achieving stable cell operation for 50 h with a <10% drop in performance before pursuing ADT studies. As an example, we used a MEA-based electrolyzer to conduct a standard durability test (See ESI† for methods). The materials and operating conditions listed in Table 3 are those we used for this test. The benchmark performance metrics are specific product

Table 3 Standard operating procedure for running a regular ECO_2RR durability test to benchmark a cell configuration prior to the pursuit of ADT studies

Cell configuration and materials		Operating conditions	
Cell type	MEA	Cathode feed:	100% CO_2
Gas diffusion layer:	Sigracet 31BC[a]	Relative humidity:	100%
Catalyst deposition:	Spray-coating	F_{CO_2}:	17.5 mL min^{-1}
Cathode catalyst:	2 mg cm^{-2} Ag NP w/2–4 wt% Sustainion binder	P_{CO_2}:	10 psig[b]
Anode catalyst:	IrO_2	$F_{electrolyte}$:	1 mL min^{-1}
Catholyte:	N/A	Catholyte recycling:	N/A
Anolyte:	0.1 M $KHCO_3$	Anolyte recycling:	Yes
Membrane:	Sustainion 37-50 AEM	Temperature:	25 °C
		Pressure:	1 atm
		Applied current density:	−200 mA cm^{-2}

Pre-testing characterization and preparation
1. **SEM EDS/EDX.** Take SEM images of the entire cathode at least from a top view. The voltage may vary, but use magnifications around 25×, 1000×, and 10 000× to obtain pictures of the catalyst layer as a whole along with layer morphology. At the median magnification, collect an EDS/EDX map of the cathode surface
2. **Solid state XRF**. Measure XRF of the cathode to collect information on catalyst layer composition as a reference for post-test characterization
3. **Prepare electrolyte**. Dissolve enough electrolyte salt in deionized (>18 mΩ cm) water to get at least 250 mL of electrolyte and cool to room temperature before continuing
4. **Electrolyte XRF**. Measure XRF of the electrolyte to check the electrolyte for impurities and to obtain a reference for post-test characterization
Pre-testing conditioning and preparation
5. **Soak membrane**. If using a membrane, be sure it has been properly conditioned prior to use. The anion exchange membrane should be soaked in 1 M KOH for at least 24 h
6. Electrode conditioning. Soak cathode in 1 M KOH for 1 h to exchange Cl^- ions in Sustainion with OH^-
7. **Assemble cell**. Put cell together using cathode, anode, membrane, gasket(s), flow chambers, current collectors, and tubing
Pre-testing electrochemical conditioning
8. **LSV** (if using easily oxidized catalyst). Run an LSV from 0 to −0.40 V *vs.* RHE to get rid of any oxides that might be present in the catalyst layer
Pre-testing electrochemical characterization
10. **Potentiostatic EIS**. Conduct an EIS experiment to measure cell and charge resistance. Set the cathode potential to −0.25 V *vs.* RHE and the frequency range at 10 kHz to 0.1 Hz
Durability test
11. Begin applying the current
12. Wait for the cell potential to equilibrate and for effluent gas to fill volume from cell through GC
13. Take the first GC injection. This marks $t = 0$. Ensure the FE of the main product is at expected value
14. Set GC to take an injection every hour or manually take injection every hour while applying current for a total of 50 h. Collect individual electrode potential data every hour as well, if possible
15. Stop applying the current, but **do not** disassemble cell or disconnect
Post-testing electrochemical characterization
16. **Potentiostatic EIS**. Conduct an EIS experiment to measure cell and charge resistance. Set the cathode potential to −0.25 V *vs.* RHE and the frequency range at 10 kHz to 0.1 Hz. Afterwards, disassemble cell being careful not damage the cathode
Post-testing characterization
18. **SEM EDS/EDX.** Take SEM images of the entire electrode at least from a top view. Be sure to use the same conditions and magnifications as the initial SEM images. At the median magnification, collect an EDS/EDX map of the cathode surface
19. **Solid state XRF**. Measure XRF of the electrode using the same conditions as the pre-testing measurements
20. **Electrolyte XRF**. Measure XRF of the electrolyte using the same conditions as the pre-testing measurements
21. **Mass balance**. Using GC data from the entire testing period, complete carbon mass balances to determine CO_2 crossover across the membrane and CO_2 conversion at the cathode

[a] Sigracet 31BC has since been discontinued and has been replaced with Sigracet 39BB in our experiments. [b] CO_2 pressure can vary; should represent value needed to maintain proper pressure balance within cell.

faradaic efficiency, which should start at >80%, and cell potential (energy efficiency), which are reported in Fig. 6. We also include CO_2 crossover into the electrolyzer, a common issue with flow-based electrolyzers, and CO_2 conversion. The FE_{CO} remains stable over the 50 h of testing, staying between 96% and 99% and well within our <10% performance drop goal. Fig. 6b highlights the cell potential over time, which hovers around -2.92 ± 0.02 V throughout testing (complete graph in ESI†). The CO_2 conversion remains at ~41.5%, which reiterates the stability of the catalyst and MEA depicted by the FE_{CO}.

When completing this benchmark test or accelerated studies (discussed next), one should be sure to report these metrics and compare them to our durability study here. One should list all materials, operating conditions, and acceleration methods utilized for proper comparison as well.

4.2 Proposed ECO_2RR acceleration methods

4.2.1 Current and total charge. When conducting a normal ECO_2RR durability test, researchers typically choose a constant

Table 4 Details and instructions for the proposed accelerated durability testing protocol for ECO_2RR systems. The top portion explains the operating conditions for the experiment and the bottom portion specifies characterization techniques for monitoring the performance and degradation of the system as a whole

	Values		
Operating conditions	Base case (benchmark)	Accelerated case 1	Accelerated case 2
Current density	200 mA cm^{-2}	500 mA cm^{-2}	1 A cm^{-2}
Experiment time (simulated time)	50 h	20 h (50 h)	10 h (50 h)
Cycle type and duration (optional)	None		
CO_2 stream relative humidity	100%		
CO_2 stream contaminants	None		
Electrolyte(s)	0.1 M $KHCO_3$		
Temperature	25 °C		
Pressure	1 atm		

Suggested metrics	Characterization method	Frequency of measurement	Failure mode(s) to observe
Cell potential	Potentiostat	Every 30 min	All
Faradaic efficiency of main product(s)	Gas chromatograph and/or ^1H NMR	Every 30 min	
Electrode morphology	SEM Micro-CT	Before and after testing	Agglomeration Leaching
Cell resistance	EIS	Before and after testing	All
Electrolyte composition	^{19}F NMR XRF ICP-OES	Every 30 min	Binder dissolution Leaching
ECSA	CV	Before and after testing	Agglomeration Leaching
Electrode composition	XPS EDS/EDX XRF	Before and after testing	Poisoning Carbonate formation Binder dissolution
CO_2 conversion	GC and mass balance	During testing	All
CO_2 crossover	GC and mass balance	During testing	Membrane failure

current (or potential) to run their cell at. In addition, researchers can choose a total time to run for or simply record how long the system lasts. Using these parameters and data, one can then determine the total charge passed (coulombs) throughout an entire durability experiment. Then, the same total charge can be passed using a shorter timescale while applying a higher current density. For example, if one were to perform an experiment where a current density of 100 mA cm^{-2} was applied for 48 h, then the total charge passed over that time period would be 17 280 C. To accelerate that experiment and complete it in 6 h, one would hold the current at 800 mA cm^{-2} to pass the same charge across the system. This approach can

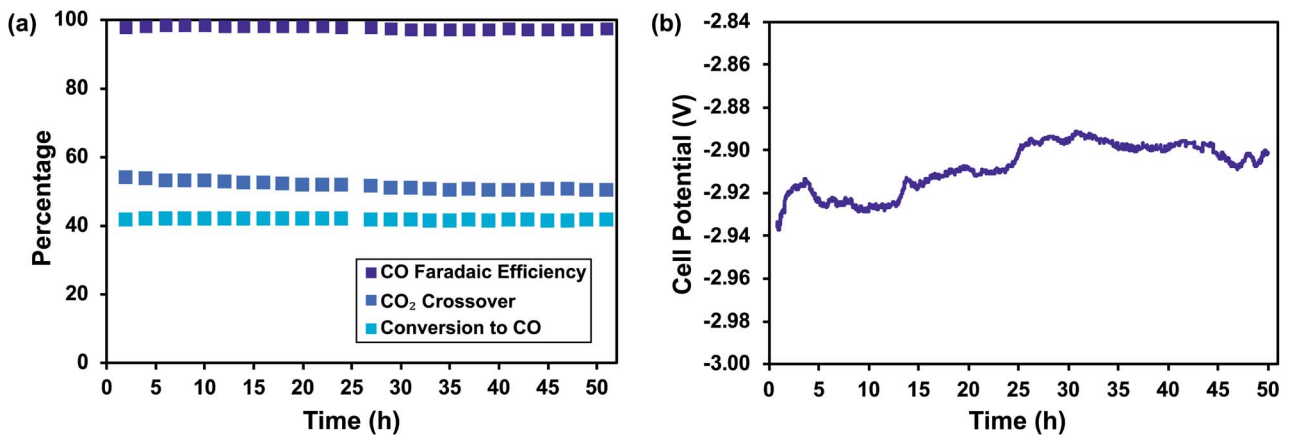

Fig. 6 Results from our 50 h, 200 mA cm^{-2} benchmark durability test conducted in a MEA-based ECO_2RR electrolyzer. (a) Carbon monoxide faradaic efficiency, CO_2 crossover through the membrane into the anolyte, and CO_2 conversion at the cathode. (b) Cell potential over 50 h of testing at −200 mA cm^{-2}.

be adopted for any cell configuration and does not require a more complex setup. Increasing current is therefore a simple acceleration method and is listed first in our suggested protocol. Unlike fuel cells (Table 2), this protocol for ECO_2RR does not focus on cycles, so cycle time is not important here; yet, we leave cycles in the protocol since cycling can be a method of accelerated stress testing, which we will briefly discuss below.

4.2.2 High temperatures and pressures. Most researchers perform ECO_2RR experiments at ambient temperatures (~25 °C) and pressures (~1 atm) because ECO_2RR does not require increased temperatures or pressures to produce significant activity. With more complicated setups, however, a few labs have explored ECO_2RR at high pressure and/or temperature,[54–61] motivated by current industrial practices. For example, the direct feed of hot flue gasses to a ECO_2RR cell from CO_2 point sources (at ~20–350 °C and ambient pressure) has been explored to offset costs related to purifying the CO_2 feed stream, while at the same time possibly accelerating the ECO_2RR process.[61–63]

Prior work has shown that increasing pressure improves overall ECO_2RR activity and faradaic efficiency towards CO, formate, and hydrocarbons.[54,55,57,58,61] Higher operating temperatures reduce energy requirements (cell voltage).[61] Nonetheless, temperature influences product selectivity: higher temperatures led to an increase in H_2 production.[56,60,61] Also, CO_2 solubility in aqueous electrolytes is affected, with a small trade-off: increasing pressure improves CO_2 solubility, while increasing temperature does the opposite. Further studies of ECO_2RR as a function of temperature and pressure are ongoing. Ultimately, altering temperature and/or pressure offers two other means of accelerating system degradation.

Suggesting specific temperature and pressure ranges becomes difficult since the field lacks studies that report the exact rate constant of ECO_2RR to a certain product and its dependence on these parameters. Yet, one can infer an exponential relationship between temperature and ECO_2RR activity by using the Arrhenius equation and assuming most of the intermediate steps for ECO_2RR to be endothermic.[64,65] As for the relationship with pressure, one can make assumptions based on classical kinetics including equilibrium constants and Le Chatelier's Principle. Like increasing current, increasing temperature and pressure can trigger degradation over shorter time scales due to increased activity, and so we include both as operating conditions in Table 4, using room temperature and pressure as baseline values.

4.2.3 CO_2 feed contaminants. Contaminants in the ECO_2RR feed stream can cause poisoning and fouling of the electrode, as well as electrode corrosion and electrolyte degradation. When considering the gaseous feed stream, most modern industrial processes emit CO_2 as a side product along with other gases (*i.e.,* flue gas), usually at high temperatures and/or pressures as mentioned previously. The exact composition and concentrations of the flue gas will depend on the CO_2 point source (*e.g.*, cement and steel plants, petroleum refining, and power plants).[66] Yet, we can expect a combination of water vapor/droplets (humidity), N_2, NO_x, SO_x, hydrocarbons, H_2S, *etc.* (contaminants) mixed within the CO_2.[66] Stream impurities such as SO_x and NO_x can be detrimental to ECO_2RR as they can poison the cathode catalysts, although further studies need to be conducted to fully understand their effects.[67,68] Therefore, the presence of stream contaminants would expectedly trigger faster degradation rates. For this protocol, however, we state the use of CO_2 streams without impurities to maintain simplicity for lab setup sake.

4.2.4 Electrolyte feed. In a laboratory setup for ECO_2RR, aqueous electrolytes are prepared using salts that typically contain trace metals despite their purity. When using electrolytes at scale, these metal impurities only become more problematic. Some of these electrolyte impurities can poison the catalyst, thus harming ECO_2RR. Using electrolyte salt impurity as an acceleration method is tricky though since most researchers purchase commercial salts for ECO_2RR; the impurity composition can vary significantly between batches and different electrolytes chosen, making it difficult to control and monitor across various ADT experiments and labs. As a result, for the proposed protocol we leave the choice of electrolyte to the researcher but suggest electrochemically purifying or chelating the solution prior to running the accelerated test.[69,70] If desired, researchers can artificially create and therefore control impurities in commercial electrolytes to study their effects.

Electrolyte ions also can cause degradation of the electrode and/or membrane materials. Highly concentrated electrolytes are used because they improve overall ECO_2RR activity through increased conductivity which helps shuttle ions between the cathode and anode. Also, the cations and anions in the electrolyte as well as electrolyte pH have shown to play a role in stabilizing ECO_2RR intermediates and/or influencing product selectivity.[18,29] Yet, high molarity of certain ions may accelerate degradation by further dissolving the binder and/or corroding the catalyst. Moreover, increasing the molarity of some salts may result in an increase or decrease in electrolyte pH, possibly leading to conditions that are too harsh for the electrode/system materials. If using a hydroxide-based electrolyte, increased concentration can also enhance carbonate formation (eqn (2)). As stated in Section 2, hydroxide ions can also attack the fluorinated binders that keep the electrode together.[30] Consequently, increasing electrolyte molarity can be used as an approach to accelerate degradation.

We should state that both overall electrolyte molarity and impurities become relevant when considering directly feeding seawater as the electrolyte to lower process costs. Some ECO_2RR labs have begun investigating using seawater as an electrolyte.[11,71] Also, corrosion studies have been conducted to understand the effect of seawater on the lifetime of metals and alloys such as stainless steel,[72] often used as the current collector for ECO_2RR cells.

Newer tests for ECO_2RR have been conducted in SOECs, which do not require an aqueous electrolyte.[19,51] Therefore, the aforementioned electrolyte feed acceleration methods would not apply to SOECs. The other acceleration methods mentioned in the protocol are more suitable for a SOEC setup.

4.2.5 Feed humidity. CO_2 stream humidity is another element in our ADT protocol since different humidity levels too

can prompt and accelerate degradation.[14,73] For regular accelerated tests, one would omit humidifying CO_2, but again it becomes very relevant when considering industrial CO_2 feeds. Humidified CO_2 streams are used for MEA-based CO_2 electrolyzers and SOECs, since they characteristically do not use a liquid electrolyte at the cathode.[10,19,52,74] Though, having water in the CO_2 stream can still promote degradation mechanisms such as binder dissolution, catalyst restructuring, and carbonate formation (to various extents depending on the humidity level). Moreover, as we saw in Section 3, one can switch between a dry and humidified CO_2 feed in a polymer electrolyte/membrane electrode assembly fuel cell to observe membrane degradation or other effects.[43]

4.2.6 Stress testing *via* cycling. In Section 4.1.1, we mentioned potential or current cycling as an accelerated stress testing method. With this, the potential or current is repeatedly ramped up and down (in step or triangular patterns) between two set values. In fuel cell research, cycling is used mimic start/stop operation in its application for transportation. In ECO_2RR research, cycling can mimic variable loads. Essentially, cycling reveals how stable and robust an electrode (or a system) is under extreme conditions.

4.3 Characterization of failure modes

As with regular durability tests, system and component characterization can be done before, during, and after accelerated durability testing to give a sufficient picture of how and when failure occurs.[28] Ideally though, a ECO_2RR ADT would be combined with an *in situ* characterization technique, such as Raman spectroscopy, to obtain real time degradation data during the experiment. Some labs have already manufactured *in situ* spectroscopy cells to obtain mechanistic insights.[75] Examining Section 3, we can come up with the best methods and steps for observing failure modes if they occur. The methods listed in the table, such as SEM, energy-dispersive X-ray spectroscopy (EDX/EDS), and XPS should be conducted prior to running the accelerated test to get a complete picture of electrode composition and morphology. Moreover, measuring both cell resistance *via* EIS and ECSA *via* CV before running the ADT tells how well the cell passes charge and reveals active site availability on the electrode, respectively.[76] Pb underpotential deposition (UPD) is a more accurate method for measuring ECSA, but renders the electrode useless as remnant Pb poisons the catalysts layer prior to use. CV is a much simpler technique that gives a sufficient estimate of ECSA.

During accelerated testing, it is important to monitor the cell potential specific to ECO_2RR; if over time HER, which requires lower potentials, takes over, then the cell potential (absolute value) decreases and may correspond to a deceptive improvement in energy efficiency. Along those lines, the FE of the main ECO_2RR product of interest is monitored constantly as it is the main cue for the inception of one or more failure modes. Finally, if an aqueous electrolyte is being utilized (unlike SOECs), collecting samples for performing analysis in addition to ^1H NMR (for product quantification) such as ^{19}F NMR, X-ray fluorescence (XRF), and inductively coupled plasma optical emission spectrometry (ICP-OES) would verify the issues of binder dissolution and catalyst leaching. As discussed in Section 3, some catalyst layer binders are fluorinated polymers,

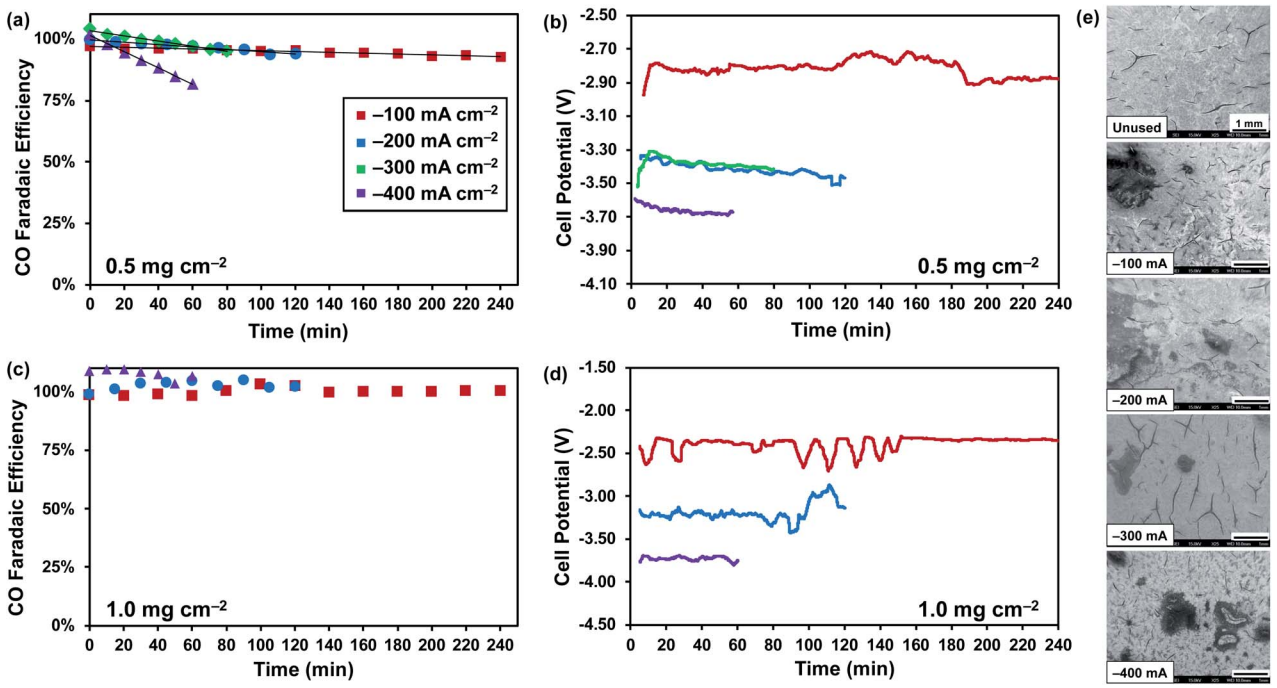

Fig. 7 Carbon monoxide faradaic efficiency and cell potential plots for each case in the total charge passed ECO_2RR accelerated test conducted in an alkaline flow electrolyzer. (a and b) 0.5 mg cm^{-2} Ag cathode and (c and d) the 1 mg cm^{-2} Ag cathode. The legend is the same for all images. (e) SEM images on the far right show the surface of the 0.5 mg cm^{-2} Ag electrodes before (unused) and after testing under each current density.

and therefore ^{19}F NMR can be used to measure any free F^- ions and C–F_x bonds, similar to work performed by Lim *et al.*[43] If any catalyst nanoparticles are coming off of the layer and leaching into the electrolyte, then either XRF or ICP-OES measurements would detect trace concentrations of metal in the solution.

Once the ADT has been finished, performing the same techniques from before running the test will reveal or further validate failures in the catalyst layer: agglomeration from SEM and ESCA measurements, leaching from SEM, and binder dissolution, poisoning, and carbonate formation from XPS or EDS.[41,42,44] The final EIS measurement will depict the communal effect of these failure mechanisms on the cell, like current density and FE do as well. Using the collected GC peak data, a mass balance can be performed to calculate the CO_2 conversion and CO_2 crossover into the electrolyte.

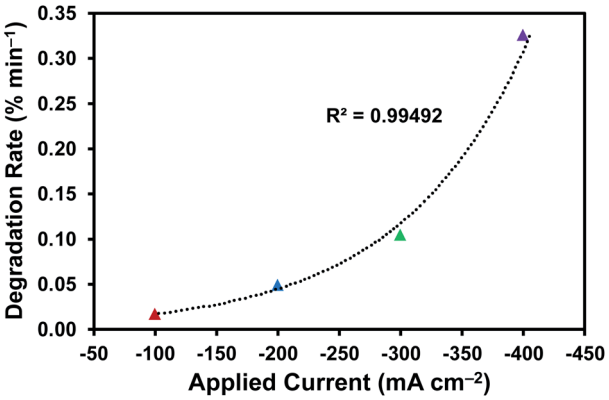

Fig. 8 Plot of degradation rate *vs.* the applied current density revealing an exponential relationship.

4.4 ECO_2RR ADT protocol validation

In the absence of thorough accelerated degradation and durability studies in the ECO_2RR field, it is difficult to verify the ADT approaches presented here. Thus, we collected our own experimental data for validation of two acceleration methods: (1) passing the same total charge over different time periods and (2) increasing electrolyte molarity. In all tests, we used a Ag cathode of varying loading, and a 1 mg cm^{-2} IrO_2 anode in an alkaline flow electrolyzer reported earlier (ESI†).[29]

4.4.1 Validation of total charge passed method. For our base case, we held the current density at −100 mA cm^{-2} for 4 h (equalling a total passed charge of 1440 C). We then created two accelerated cases by doubling (−200 mA cm^{-2}) and then quadrupling (−400 mA cm^{-2}) the current density, therefore cutting the observation time by 2 (2 h total) and 4 (1 h total), respectively. All three experiments were carried out once with a 1 mg cm^{-2} Ag cathode and then with a 0.5 mg cm^{-2} Ag cathode to determine whether loading had an effect on degradation rate, as perceived by Siracusano *et al.* for water electrolysis.[34] An additional accelerated case (−300 mA cm^{-2}, $1\frac{1}{3}$ h) was carried out with the 0.5 mg cm^{-2} Ag cathode as well.

The 1 mg cm^{-2} Ag cathode did not exhibit any major performance degradation (in FE_{CO} or cell potential) when tested in both base and accelerated cases (Fig. 7). This result is likely due to the high cathode loading in combination with the short experimental time relative to durability tests done in the past.[77,78] The results we obtained when running the 0.5 mg cm^{-2} Ag cathode further support this conclusion as the FE_{CO} decreases in all four cases over the testing period (Fig. 7a). Data from pre- and post-test SEM revealed that carbonate formation contributed to the drop in performance (Fig. 7e). In each case, the average cell potential (Fig. 7b) did not alter significantly during the experiment time, confirming that the cell potential is a sensitive metric as any changes may correspond to increased rates of HER and not to better energetic efficiency. Complete cell potential graphs are provided in the ESI (Fig. S3†).

Looking closer at Fig. 7a, we noticed that each applied current density degrades the 0.5 mg cm^{-2} Ag cathode at a different rate; the degradation rate here is defined as the slope of the linear fit for the FE_{CO} plot. Plotting the degradation rate/slope for each case *vs.* the applied current density reveals an exponential relationship between the two (Fig. 8). These differences in the degradation rates are likely linked to Butler–Volmer kinetics; current density and cell (or cathode) potential are known to possess an exponential relationship.[79] The higher cell potentials needed to sustain each applied current density lead to an increase in rate of degradation (Table S3†). Moreover, increased activity produces higher amounts of OH^- and product gas bubbles, which encourages carbonate formation and can physically erode the catalyst surface, respectively.[28]

4.4.2 Validation of electrolyte molarity method. The base case for electrolyte molarity tests was the same for that of the total charge passed: −100 mA cm^{-2} for 4 h with 1 M KOH. In the accelerated cases, the cell was also subjected to −100 mA cm^{-2} for 4 h, but the electrolyte molarity was increased to 2 M, 4 M, and 8 M KOH. Here, the Ag cathode loading was 0.5 mg cm^{-2}.

Increasing the concentration of the KOH electrolyte does improve the overall kinetics and energy efficiency of our ECO_2RR flow electrolyzer, but only to a certain point. The CO faradaic efficiency and the cell potential for all cases are displayed in Fig. 9. When increasing [KOH] from 1 M to 2 M, we observed a decrease (less negative) in cell potential, and the FE_{CO} is stable at ∼100% throughout the 4 h of testing. Even though 1 M KOH is a less harsh electrolyte, we measured a slight decrease in the FE_{CO} because the average cell potential was higher than that when using 2 M KOH. As in Section 4.3.1, this effect can be explained by Butler–Volmer kinetics. When moving from 2 M to 4 M and 8 M KOH, we begin to see a detrimental effect on the FE_{CO}; within 2 h for 4 M KOH and 40 min for 8 M KOH, the CO FE begins to drop off from its starting value. The FE_{CO} drops to 0% in about 3 h when using 8 M KOH as an electrolyte. These results can be explained *via* cell potential plots (Fig. 9b and S4†). The average cell potential for the 1 M KOH case is about −2.80 V and just by switching to 2 M KOH, we improved to ∼ −2.35 V. Surprisingly, the cell potential did not further improve when using the 4 M and 8 M KOH, suggesting that we reached a limiting electrolyte conductivity in our system. Once we passed this limiting conductivity, the high [OH^-] and alkalinity took their toll on the Ag cathode by way of binder dissolution, catalyst leaching, and

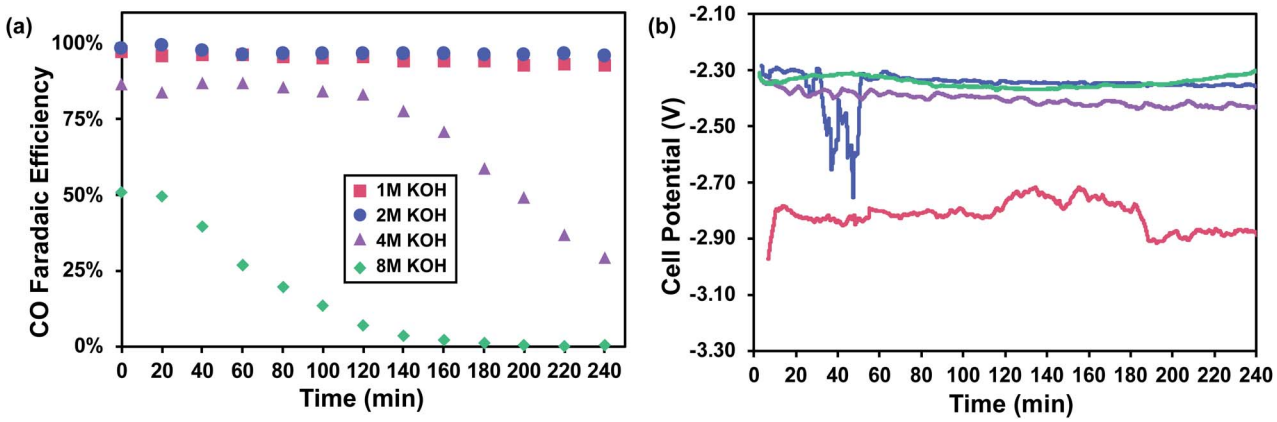

Fig. 9 Results from the electrolyte molarity ECO_2RR acceleration test conducted in an alkaline flow electrolyzer. (a) The faradaic efficiency of CO and (b) cell potential over 4 hours of testing. The legend is the same for both images.

carbonate formation, all of which we determined from post-test SEM images (Fig. S5†). The catalyst surface is covered in dark [carbonate] patches, and the catalyst layer has begun to detach from the GDL. As mentioned before in Section 2, high amounts of OH^- shift the equilibrium in the carbonate formation reaction (eqn (2) and (3)) and degrades the fluorinated polymers often used as the binder. Once the binder fails, then the Ag in the cathode is much more susceptible to leaching.

Our attempt to validate a few of the methods from the ADT protocol is only a first step to understanding accelerated degradation trends and relationships for ECO_2RR. Moving forward, a full study should be done examining each operating condition as an accelerated condition and how they relate to base case durability and degradation studies. Of course, all of the values and characterization methods listed in Table 4 can be changed and manipulated to better serve a specific cell, purpose, or aspect of an ECO_2RR system. Specifically, we would also consider membrane degradation and delamination as failure modes when testing with a MEA-based cell or a SOEC. Again, the DOE has provided multiple fuel cell protocols, each for a different component of the fuel cell. Yet, having one general ECO_2RR protocol becomes beneficial when comparing the durability of systems and cells across various labs.

5. Conclusions

The electrochemical reduction of CO_2 is projected (based on technoeconomic and life cycle analyses) to hold promise for combatting CO_2 emissions by using CO_2 as a feedstock and replacing highly carbon positive processes in the manufacturing of chemicals and fuels. The field has rapidly grown and taken massive steps toward satisfying several performance metrics required for industrial feasibility. Yet, insufficient durability of electrodes as well as cell configurations and associated operating conditions has been identified as a prominent roadblock standing in the way of application at scale. Once the ECO_2RR field as a whole achieves longer system lifetimes (*i.e.*, <10% performance drop over >48 h), then accelerated durability testing becomes necessary as a way to determine a system's lifetimes in a shorter amount of time.

To date very few accelerated durability and stress studies have been reported for ECO_2RR, but other electrochemical technology fields (fuel cell, water electrolysis, and chlor-alkali electrolysis) have long since employed ADTs and ASTs to study systems and system components for long-term robustness. Conducting a detailed review of ADTs/ASTs for these other electrochemical applications provided guidance for the ECO_2RR ADT approaches proposed here. Before beginning ADT studies on ECO_2RR systems, researchers should benchmark their systems to ensure they meet standard durability (50 h) at high activity ($\geq$200 mA cm^{-2}) and product selectivity (>80%).

To validate some of the proposed ADT approaches for ECO_2RR, we conducted preliminary experiments for the total charged passed and electrolyte molarity approaches. When passing the same amount of total charge, the results revealed that the observed degradation rates exhibit an exponential trend with respect to applied current. We observed a limiting conductivity when increasing the electrolyte concentration, after which cathode degradation hastened. These tests represent an initial step toward understanding how accelerated conditions affect various ECO_2RR cells and identifying correlations for estimated lifetimes and other characteristics. We did not validate the other acceleration approaches (high T&P, feed contaminants, humidity, and cycling). Undoubtedly, several of these other approaches may find utility for standard as well as accelerated ECO_2RR durability studies.

Application of accelerated durability testing protocols only is warranted once ECO_2RR setups achieve reasonable lifetimes in un-accelerated durability testing; *e.g.*, less than 10% performance loss over 2–4 days. Also, different *in situ* or *ex situ* characterization methods should be incorporated in setups for lifetime testing. Indeed, now is the time to design and build sophisticated setups dedicated to studying both standard and accelerated durability, setups that are equipped with various analytics and characterization techniques.[80] Such test configurations not only will help understand and subsequently improve lifetime determining factors of electrode and cell design, they

will also enable the testing of ever-better configurations for resiliency under 'real-world' conditions, *e.g.*, contaminants expected to be present in CO_2 feeds from different point sources.

Conflicts of interest

There are no conflicts to declare.

Acknowledgements

The authors gratefully acknowledge Shell's New Energies Research and Technology (NERT) Dense Energy Carriers program for providing funding for this work. We would also like to acknowledge the International Institute of Carbon Neutral Energy Research (WPI-I2CNER) sponsored by the Japanese Ministry for Education, Culture, Sports, Science and Technology and the SURGE Fellowship for the funding of UON.

References

1 J. Oerlemans, *Science*, 2005, **308**, 675–677.
2 Intergovernmental Panel on Climate Change, *Climate Change 2014 Synthesis Report Summary for Policymakers*, https://www.ipcc.ch/pdf/assessment-report/ar5/syr/AR5_SYR_FINAL_SPM.pdf.
3 United States Energy Information Administration, *International Energy Outlook*, 2018, https://www.eia.gov/outlooks/ieo/.
4 *Source of Greenhouses Gases*, United States Environmental Protection Agency, 2016, https://www.epa.gov/ghgemissions/sources-greenhouse-gas-emissions.
5 J. Hansen, P. Kharecha, M. Sato, V. Masson-Delmotte, F. Ackerman, D. J. Beerling, P. J. Hearty, O. Hoegh-Guldberg, S. L. Hsu, C. Parmesan, J. Rockstrom, E. J. Rohling, J. Sachs, P. Smith, K. Steffen, L. Van Susteren, K. von Schuckmann and J. C. Zachos, *PLoS One*, 2013, **8**, e81648.
6 H. R. Jhong, S. C. Ma and P. J. A. Kenis, *Curr. Opin. Chem. Eng.*, 2013, **2**, 191–199.
7 Y. Hori, *Modern Aspects of Electrochemistry*, 2008, pp. 89–189, DOI: 10.1007/978-0-387-49489-0.
8 S. Verma, U. O. Nwabara and P. J. A. Kenis, *Nanostruct. Sci. Technol.*, 2019, 219–251, DOI: 10.1007/978-3-319-92917-0_10.
9 S. C. Ma, M. Sadakiyo, R. Luo, M. Heima, M. Yamauchi and P. J. A. Kenis, *J. Power Sources*, 2016, **301**, 219–228.
10 R. B. Kutz, Q. M. Chen, H. Z. Yang, S. D. Sajjad, Z. C. Liu and I. R. Masel, *Energy Technol.*, 2017, **5**, 929–936.
11 K. Nakata, T. Ozaki, C. Terashima, A. Fujishima and Y. Einaga, *Angew. Chem., Int. Ed.*, 2014, **53**, 871–874.
12 S. Verma, B. Kim, H. Jhong, S. C. Ma and P. J. A. Kenis, *ChemSusChem*, 2016, **9**, 1972–1979.
13 M. Jouny, W. Luc and F. Jiao, *Ind. Eng. Chem. Res.*, 2018, **57**, 2165–2177.
14 A. J. Martin, G. O. Larrazabal and J. Perez-Ramirez, *Green Chem.*, 2015, **17**, 5114–5130.
15 B. Kim, F. Hillman, M. Ariyoshi, S. Fujikawa and P. J. A. Kenis, *J. Power Sources*, 2016, **312**, 192–198.
16 M. Asadi, K. Kim, C. Liu, A. V. Addepalli, P. Abbasi, P. Yasaei, P. Phillips, A. Behranginia, J. M. Cerrato, R. Haasch, P. Zapol, B. Kumar, R. F. Klie, J. Abiade, L. A. Curtiss and A. Salehi-Khojin, *Science*, 2016, **353**, 467–470.
17 F. W. Li, L. Chen, G. P. Knowles, D. R. MacFarlane and J. Zhang, *Angew. Chem., Int. Ed.*, 2017, **56**, 505–509.
18 C. T. Dinh, T. Burdyny, M. G. Kibria, A. Seifitokaldani, C. M. Gabardo, F. P. G. de Arquer, A. Kiani, J. P. Edwards, P. De Luna, O. S. Bushuyev, C. Q. Zou, R. Quintero-Bermudez, Y. J. Pang, D. Sinton and E. H. Sargent, *Science*, 2018, **360**, 783–787.
19 M. H. Zheng, S. Wang, Y. Yang and C. R. Xia, *J. Mater. Chem. A*, 2018, **6**, 2721–2729.
20 T. Haas, R. Krause, R. Weber, M. Demler and G. Schmid, *Nat. Catal.*, 2018, **1**, 32–39.
21 J. Kurtz, H. Dinh, G. Saur and C. Ainscough, *Fuel Cell Technology Status Analysis*, https://www.nrel.gov/hydrogen/fuel-cell-technology-status.html, accessed July 28, 2018.
22 Z. Weng, X. Zhang, Y. S. Wu, S. J. Huo, J. B. Jiang, W. Liu, G. J. He, Y. Y. Liang and H. L. Wang, *Angew. Chem., Int. Ed.*, 2017, **56**, 13135–13139.
23 H. Wang, J. Jia, P. F. Song, Q. Wang, D. B. Li, S. X. Min, C. X. Qian, L. Wang, Y. F. Li, C. Ma, T. Wu, J. Y. Yuan, M. Antonietti and G. A. Ozin, *Angew. Chem., Int. Ed.*, 2017, **56**, 7847–7852.
24 F. W. Li, M. Q. Xue, G. P. Knowles, L. Chen, D. R. MacFarlane and J. Zhang, *Electrochim. Acta*, 2017, **245**, 561–568.
25 J. L. Liu, C. X. Guo, A. Vasileff and S. Z. Qiao, *Small Methods*, 2017, **1**.
26 H. S. Jeon, S. Kunze, F. Scholten and B. Roldan Cuenya, *ACS Catal.*, 2018, **8**, 531–535.
27 C. Rogers, W. S. Perkins, G. Veber, T. E. Williams, R. R. Cloke and F. R. Fischer, *J. Am. Chem. Soc.*, 2017, **139**, 4052–4061.
28 U. O. Nwabara, E. R. Cofell, P. J. A. Kenis, S. Verma and E. Negro, *ChemSusChem*, 2020, **13**, 855–875.
29 S. Verma, X. Lu, S. C. Ma, R. I. Masel and P. J. A. Kenis, *Phys. Chem. Chem. Phys.*, 2016, **18**, 7075–7084.
30 M. F. Rabuni, N. M. N. Sulaiman, M. K. Aroua and N. A. Hashim, *Ind. Eng. Chem. Res.*, 2013, **52**, 15874–15882.
31 K. G. Schulz, U. Riebesell, B. Rost, S. Thoms and R. E. Zeebe, *Mar. Chem.*, 2006, **100**, 53–65.
32 United States Department of Energy, *Cell Component Accelerated Stress Test and Polarization Curve Protocols for PEM Fuel Cells*, https://www.energy.gov/sites/prod/files/2015/08/f25/fcto_dwg_usdrive_fctt_accelerated_stress_tests_jan2013.pdf.
33 C. Takei, K. Kakinuma, K. Kawashima, K. Tashiro, M. Watanabe and M. Uchida, *J. Power Sources*, 2016, **324**, 729–737.
34 S. Siracusano, N. Hodnik, P. Jovanovic, F. Ruiz-Zepeda, M. Sala, V. Baglio and A. S. Arico, *Nano Energy*, 2017, **40**, 618–632.
35 Y. J. Leng, G. Chen, A. J. Mendoza, T. B. Tighe, M. A. Hickner and C. Y. Wang, *J. Am. Chem. Soc.*, 2012, **134**, 9054–9057.
36 P. Paciok, M. Schalenbach, M. Carmo and D. Stolten, *J. Power Sources*, 2017, **365**, 53–60.

37 M. Sugiyama, K. Saiki, A. Sakata, H. Aikawa and N. Furuya, *J. Appl. Electrochem.*, 2003, **33**, 929–932.
38 I. Moussallem, J. Jorissen, U. Kunz, S. Pinnow and T. Turek, *J. Appl. Electrochem.*, 2008, **38**, 1177–1194.
39 A. Sakata, M. Kato, K. Hayashi, N. Furuya, H. Aikawa and K. Saiki, *J. Electrochem. Soc.*, 1999, **99**, 223–233.
40 T. Morimoto, K. Suzuki, T. Matsubara and N. Yoshida, *Electrochim. Acta*, 2000, **45**, 4257–4262.
41 K. Vaarmets, S. Sepp, J. Nerut and E. Lust, *ECS Trans.*, 2016, **75**, 899–911.
42 F. Y. Zhang, S. G. Advani, A. K. Prasad, M. E. Boggs, S. P. Sullivan and T. P. Beebe, *Electrochim. Acta*, 2009, **54**, 4025–4030.
43 C. Lim, L. Ghassemzadeh, F. Van Hove, M. Lauritzen, J. Kolodziej, G. G. Wang, S. Holdcroft and E. Kjeang, *J. Power Sources*, 2014, **257**, 102–110.
44 N. Wagner, M. Schulze and E. Gulzow, *J. Power Sources*, 2004, **127**, 264–272.
45 P. Costamagna and S. Srinivasan, *J. Power Sources*, 2001, **102**, 253–269.
46 M. Sudoh, T. Kondoh, N. Kamiya, T. Ueda and K. Okajima, *J. Electrochem. Soc.*, 2000, **147**, 3739–3744.
47 United States Department of Energy-National Energy Technology Laboratory, *CO_2 Utilization Focus Area*, https://www.netl.doe.gov/research/coal/carbon-storage/research-and-development/co2-utilization.
48 United States Department of Energy - Office of Energy Efficiency and Renewable Energy, Water Electrolysis Working Group, https://www.energy.gov/eere/fuelcells/water-electrolysis-working-group.
49 F. R. Brushett, M. S. Thorum, N. S. Lioutas, M. S. Naughton, C. Tornow, H. R. Jhong, A. A. Gewirth and P. J. A. Kenis, *J. Am. Chem. Soc.*, 2010, **132**, 12185–12187.
50 A. S. Kishi, S. Sayoko and M. Umeda, *J. Power Sources*, 2012, **197**, 88–92.
51 Y. M. Xie, J. Xiao, D. D. Liu, J. Liu and C. H. Yang, *J. Electrochem. Soc.*, 2015, **162**, F397–F402.
52 H. Z. Yang, J. J. Kaczur, S. D. Sajjad and R. I. Masel, *J. CO2 Util.*, 2017, **20**, 208–217.
53 T. F. O'Brien, T. V. Bommaraju and F. Hine, *Handbook of Chlor-alkali Technology*, Springer, Boston, MA, 2005.
54 C. M. Gabardo, A. Seifitokaldani, J. P. Edwards, C. T. Dinh, T. Burdyny, M. G. Kibria, C. P. O'Brien, E. H. Sargent and D. Sinton, *Energy Environ. Sci.*, 2018, **11**, 2531–2539.
55 K. Hara, A. Tsuneto, A. Kudo and T. Sakata, *J. Electrochem. Soc.*, 1994, **141**, 2097–2103.
56 T. Mizuno, K. Ohta, A. Sasaki, T. Akai, M. Hirano and A. Kawabe, *Energy Sources*, 1995, **17**, 503–508.
57 M. Todoroki, K. Hara, A. Kudo and T. Sakata, *J. Electroanal. Chem.*, 1995, **394**, 199–203.
58 R. Kas, R. Kortlever, H. Yilmaz, M. T. M. Koper and G. Mul, *ChemElectroChem*, 2015, **2**, 354–358.
59 N. Sonoyama, M. Kirii and T. Sakata, *Electrochem. Commun.*, 1999, **1**, 213–216.
60 S. T. Ahn, I. Abu-Baker and G. T. R. Palmore, *Catal. Today*, 2017, **288**, 24–29.
61 E. J. Dufek, T. E. Lister, S. G. Stone and M. E. McIlwain, *J. Electrochem. Soc.*, 2012, **159**, F514–F517.
62 B. Kim, S. Ma, H. R. M. Jhong and P. J. A. Kenis, *Electrochim. Acta*, 2015, **166**, 271–276.
63 A. Samanta, A. Zhao, G. K. H. Shimizu, P. Sarkar and R. Gupta, *Ind. Eng. Chem. Res.*, 2012, **51**, 1438–1463.
64 C. N. Cui, J. Y. Han, X. L. Zhu, X. Liu, H. Wang, D. H. Mei and Q. F. Ge, *J. Catal.*, 2016, **343**, 257–265.
65 R. Ahmad and A. K. Singh, *J. Mater. Chem. A*, 2018, **6**, 21120–21130.
66 P. Bains, P. Psarras and J. Wilcox, *Prog. Energy Combust. Sci.*, 2017, **63**, 146–172.
67 Y. Zhai, L. Chiachiarelli and N. Sridhar, *ECS Trans.*, 2009, **19**, 1–13.
68 W. Luc, B. H. Ko, S. Kattel, S. Li, D. Su, J. G. Chen and F. Jiao, *J. Am. Chem. Soc.*, 2019, **141**(25), 9902–9909.
69 Y. Hori, H. Konishi, T. Futamura, A. Murata, O. Koga, H. Sakurai and K. Oguma, *Electrochim. Acta*, 2005, **50**, 5354–5369.
70 A. Wuttig and Y. Surendranath, *ACS Catal.*, 2015, **5**, 4479–4484.
71 C. Y. Lee and G. G. Wallace, *J. Mater. Chem. A*, 2018, **6**, 23301–23307.
72 M. Schumacher, *Seawater corrosion handbook*, Noyes Data Corp., Park Ridge, N.J., 1979.
73 Y. K. Tao, S. D. Ebbesen and M. B. Mogensen, *J. Power Sources*, 2016, **328**, 452–462.
74 Y. Hori, H. Ito, K. Okano, K. Nagasu and S. Sato, *Electrochim. Acta*, 2003, **48**, 2651–2657.
75 K. G. Schmitt and A. A. Gewirth, *J. Phys. Chem. C*, 2014, **118**, 17567–17576.
76 E. L. Clark, J. Resasco, A. Landers, J. Lin, L. T. Chung, A. Walton, C. Hahn, T. F. Jaramillo and A. T. Bell, *ACS Catal.*, 2018, **8**, 6560–6570.
77 S. Verma, Y. Hamasaki, C. Kim, W. X. Huang, S. Lu, H. R. M. Jhong, A. A. Gewirth, T. Fujigaya, N. Nakashima and P. J. A. Kenis, *ACS Energy Lett.*, 2018, **3**, 193–198.
78 T. T. H. Hoang, S. C. Ma, J. I. Gold, P. J. A. Kenis and A. A. Gewirth, *ACS Catal.*, 2017, **7**, 3313–3321.
79 A. J. Bard and L. R. Faulkner, *Electrochemical methods: fundamentals and applications*, Wiley, New York, 2nd edn, 2001.
80 *2019 Annual Merit Review and Peer Evaluation Report*, Department of Energy, Crystal City, Virginia, 2019.